

Cite this: *Nanoscale*, 2011, **3**, 4411

www.rsc.org/nanoscale

PAPER

Preparation and visible light photocatalytic activity of Ag/TiO₂/graphene nanocomposite†

Yanyuan Wen, Hanming Ding* and Yongkui Shan

Received 13th June 2011, Accepted 24th August 2011

DOI: 10.1039/c1nr10604j

Great efforts have been made to develop efficient visible light-activated photocatalysts in recent years. In this work, a new nanocomposite consisting of anatase TiO₂, Ag, and graphene was prepared for use as a visible light-activated photocatalyst, which exhibited significantly increased visible light absorption and improved photocatalytic activity, compared with Ag/TiO₂ and TiO₂/graphene nanocomposites. The increased absorption in visible light region is originated from the strong interaction between TiO₂ nanoparticles and graphene, as well as the surface plasmon resonance effect of Ag nanoparticles that are mainly adsorbed on the surface of TiO₂ nanoparticles. The highly efficient photocatalytic activity is associated with the strong adsorption ability of graphene for aromatic dye molecules, fast photogenerated charge separation due to the formation of Schottky junction between TiO₂ and Ag nanoparticles and the high electron mobility of graphene sheets, as well as the broad absorption in the visible light region. This work suggests that the combination of the excellent electrical properties of graphene and the surface plasmon resonance effect of noble metallic nanoparticles provides a versatile strategy for the synthesis of novel and efficient visible light-activated photocatalysts.

1. Introduction

Anatase TiO₂ has been considered one of the most promising photocatalysts because of its long-term thermal and chemical stability, non-toxicity, low cost, and universal applicability. However, the photocatalytic efficiency of TiO₂ using natural sunlight is currently very low. Several factors are of relevance, but two are more important: the fast recombination of photo-generated electron-hole pairs and the limited optical response only to UV light. Thus, to inhibit the recombination of photo-generated electron-hole pairs and to extend the optical absorption to visible light region are two key ways to improve the photocatalytic activity of TiO₂ under solar irradiation.

In order to extend the optical absorption of TiO₂ to the visible light region, various attempts have been made to modify TiO₂,¹ including surface deposition of noble metallic nanoparticles, photosensitization with organic dyes, polymers, and semiconductors, doping with cations and/or anions, and surface reduction treatment. Recently, the nanocomposites of TiO₂ and noble metallic nanoparticles have been intensively investigated because they can enhance the photocatalytic activity primarily by extending the optical absorption to the visible light region and increasing the number of photoexcited electrons due to the enhanced near-field amplitude.^{2–6} When a noble metallic

nanoparticle is excited by light, the oscillating electric field of the light interacts with the conduction electrons. As a result, a strong oscillation of these electrons happens when the incident photon frequency is resonant with the collective oscillation of the conduction electrons. Such resonance is called localized surface plasmon resonance (SPR) for metallic nanoparticles. By engineering the size, shape and dielectric environment of the metallic nanoparticles, their absorption and scattering properties can be flexibly tuned. Localized SPR of gold and silver nanoparticles usually results in strong and broad absorption bands in the visible light region, and thus it is exploited to develop visible light-activated photocatalysts.

Another way to increase the photocatalytic activity of TiO₂ is to retard bulk and surface recombination of photogenerated electron-hole pairs in TiO₂ during a photocatalytic process. Deposition of metals on the TiO₂ surface, formation of a composite with a narrow band gap semiconductor, usage of electron donors/acceptors and hole scavengers are the common ways. Multi-walled carbon nanotube (MWCNT) is a good candidate for scavenging of photogenerated electrons mainly because of its multiple graphene layers where electrons can flow through when in contact with TiO₂.⁷ Owing to its superior charge transport properties, graphene can be a more ideal platform for photogenerated electron scavenging than MWCNT. The coupling of graphene with TiO₂ is expected to accelerate the photogenerated charge separation in a more favorable way. In addition, graphene provides a large scaffold for anchoring various substrates owing to its large specific surface area and two-dimensional planar conjugation structure. Recently, several TiO₂/graphene nanocomposites have

Department of Chemistry, East China Normal University, 3663 North Zhongshan Road, Shanghai, 200062, China. E-mail: hmding@chem.ecnu.edu.cn; Fax: +86-21-62232414; Tel: +86-21-62238536

† Electronic supplementary information (ESI) available: See DOI: 10.1039/c1nr10604j

been prepared using different recipes and explored in photocatalysis.^{8–15} In most of cases, TiO₂ (or Degussa P25) was firstly mixed with graphene oxide (GO) in suspension or in thin films, and then GO was reduced to graphene by using UV-assisted photocatalytic reduction,^{8,11} NaBH₄ reduction,¹² or one-step hydrothermal treatment.^{9,13,14} Consequently, a TiO₂/graphene nanocomposite was formed. These TiO₂/graphene nanocomposites have been used as photocatalysts for degradation of *E. coli* bacteria,¹¹ methylene blue,¹³ and benzene vapor,¹⁴ as well as hydrogen production from photocatalytic water splitting.¹² All of these photocatalytic results supported that the incorporation of graphene onto TiO₂ efficiently enhanced the photocatalytic activity of TiO₂.

While there have been quite a few researches concerning with Ag/TiO₂,^{3–6} TiO₂/graphene,^{8–15} and even Ag/graphene^{16–20} nanocomposites used as photocatalysts, less attention has been paid to Ag/TiO₂/graphene nanocomposite. In this work, we utilize both the SPR effect of Ag nanoparticles and the excellent electrical properties of graphene to design a new visible light-activated photocatalyst. In this photocatalyst, the loading of Ag nanoparticles is expected to enhance its optical response to a wider wavelength; the introduction of graphene will not only accelerate the separation of photogenerated electron-hole pairs, but also enhance the adsorption capacity of the photocatalyst, thereby improving the photocatalytic activity of TiO₂ under visible light irradiation.

2. Experimental

2.1 Preparation of Ag/TiO₂/graphene nanocomposite

Graphite oxide (GO) was synthesized from graphite powder (SP, Sinopharm Chemical Reagent Co., Ltd.) by the modified Hummers' method,²¹ using a mixture of H₂SO₄, NaNO₃, and KMnO₄. A previous graphite oxidation procedure with H₂SO₄, K₂S₂O₈, and P₂O₅ was carried out before the synthesis of GO.²² TiO₂ sol was prepared using a mixture of Ti(OC₄H₉)₄ (98%, CR), ethanol (99.7%, AR), H₂O, and HNO₃ (65%, AR) with a molar ratio of 1 : 70 : 1.9 : 0.2. Such mixture was stirred at room temperature until a transparent sol was gotten. Then GO powder and TiO₂ sol was mixed together, ultrasonicated for 10 min, and stirred for 20 min. After that, they were transferred into a Teflon-lined stainless-steel autoclave and kept at 130 °C for 5 h, followed by cooling down to room temperature naturally. The mixture was filtered, washed with water, and then dried. A gray powder was gotten, which was proven a TiO₂/graphene nanocomposite with a mass ratio of about 10 : 1, denoted as TiO₂/G.

A half-gram of TiO₂/G was dispersed in 30 ml of water, and then 20 ml of 0.1 mol L⁻¹ AgNO₃ (99.9%, AR) aqueous solution was added to the suspension. Such mixture was stirred for 20 min, filtered, washed, and then dried. The as-prepared powder was added to 20 ml of 25 mg ml⁻¹ NaBH₄ (96%, CR) aqueous solution. The mixture was stirred at room temperature for 30 min, filtered, washed, and then dried at 60 °C, getting a nanocomposite of Ag/TiO₂/graphene, denoted as Ag/TiO₂/G.

2.2 Characterization and measurements

The crystal structure was identified with a Rigaku D/Max-RB X-ray diffractometer with Ni-filtered Cu-K α radiation ($\lambda =$

1.54056 Å). XPS experiments were carried out on a RBD upgraded PHI-5000C ESCA system (Perkin Elmer) with Mg-K α radiation ($h\nu = 1253.6$ eV) at a base pressure of 5×10^{-8} Pa. Diffuse reflectance spectra were recorded with a Shimadzu 2450 solid-state UV–vis spectrophotometer equipped with an integrating sphere diffuse reflectance accessory. Fourier transform infrared spectra were recorded from KBr pellet in a Nicolet Nexus 670 spectrophotometer with a range of 400–4000 cm⁻¹. Raman spectra were acquired using a Jobin Yvon LabRam-1B spectrographer. The excitation source was a helium-neon laser with a wavelength of 632.8 nm and an excitation power of 6 mW. The morphologies were observed using a JEOL JEM-100C II transmission electron microscope.

The photodegradation of methylene blue (MB) was carried out to evaluate the photocatalytic activity of Ag/TiO₂/G nanocomposite. Photocatalytic experiments were carried out in a homemade reactor, which was surrounded with a cooling system to keep the photocatalytic reaction system at ambient temperature. A 500 W halogen lamp with a KenKo L41 UV filter ($\lambda > 410$ nm) was used as a visible light source and fixed 10 cm away from the reaction system. The photocatalyst powder (0.1 g) was suspended in 100 mL of MB aqueous solution with a concentration of 10 mg L⁻¹ under magnetic stirring. The reaction system was firstly kept in the dark for one hour to establish an adsorption-desorption equilibrium, and then exposed to the visible light. At the desired time intervals, 5 mL aliquots from each sample were taken, followed by centrifugation and filtration to remove the photocatalyst. The supernatant was used to determine the concentration of residual dye in solution. The decolorization of MB was evaluated by measuring the change in its characteristic optical absorbance using a UV-1700 UV–vis spectrophotometer.

3. Results and discussion

3.1 Structure and morphology of Ag/TiO₂/G nanocomposite

The formation of Ag/TiO₂/G nanocomposite was confirmed by transmission electron microscopy (TEM) analysis, and its representative images are presented in Fig. 1. Fig. 1a clearly demonstrates that graphene has a crumpled layered structure composed of several stacking layers of graphene sheets. Some graphene sheets were broken into small pieces during the hydrothermal treatment process. Spherical or oval nanoparticles with sizes varying several to tens of nanometres were found deposited on the surface of the graphene sheets and are randomly distributed, as shown in Fig. 1b. As can be seen from the enlarged image at the top-right corner of Fig. 1b, the spacing of the lattice fringes is 0.35 nm, corresponding to the d-spacing of (101) crystalline plane of anatase TiO₂. Such observation suggested that TiO₂ nanoparticles are highly crystallized on the graphene sheets, but randomly orientated with their crystalline planes with respect to the graphene sheets. Fig. 1c presents a TEM image of Ag/TiO₂/G at low magnification. It can be seen that TiO₂ and Ag/TiO₂ nanoparticles are not uniformly dispersed on the surface of graphene sheets and some of them are wrapped by the graphene sheets. The relatively dark regions are ascribed to Ag nanoparticles, which are adsorbed on the surface of the TiO₂ nanoparticles. As described in the experimental section, Ag⁺ ions were introduced after the formation of TiO₂/G nanocomposite.

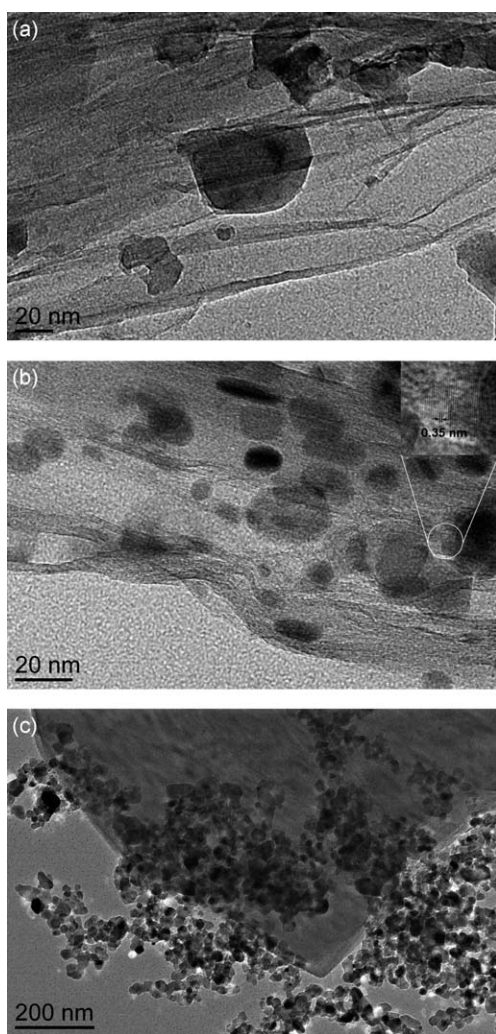


Fig. 1 TEM images of (a) graphene and (b, c) Ag/TiO₂/G at different magnifications.

These Ag⁺ ions should be preferably adsorbed on the hydrophilic surface of TiO₂, rather than the hydrophobic surface of graphene sheets. After the NaBH₄ reduction, Ag nanoparticles should be deposited on the surface of TiO₂ nanoparticles. The existence of Ag nanoparticles was further evidenced by XRD and Raman spectroscopic measurements.

The powder X-ray diffraction (XRD) pattern of the prepared Ag/TiO₂/G nanocomposite was compared with those of TiO₂/G nanocomposite and graphene oxide (GO), as depicted in Fig. 2. The XRD pattern of natural graphite (JCPDS No. 65-6212) which was used as a starting material shows a distinct diffraction peak at 26.5°, corresponding to a *d*₀₀₂ basal spacing of approximately 0.335 nm. The interlayer spacing increases to 0.702 nm for GO prepared by the oxidation of graphite according to Hummers' method, as revealed by a peak at 12.6° shown in Fig. 2a. This value falls within the range of 0.63–0.77 nm reported in the literatures. Such increment in the interlayer distance is due to the introduction of oxygen-containing functional groups generated in the oxidation process and interlamellar water molecules trapped between hydrophilic graphene oxide sheets.

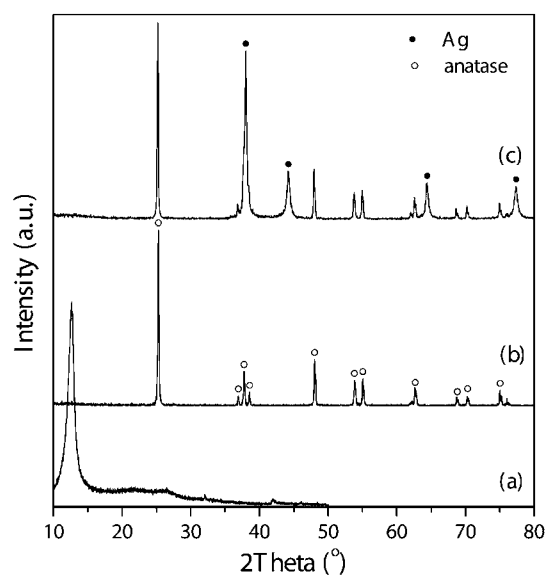


Fig. 2 XRD patterns of (a) graphene oxide, (b) TiO₂/G, and (c) Ag/TiO₂/G.

It has been previously reported that GO could be hydrothermally reduced to graphene in a sealed autoclave.^{9,13,14,23} When the mixture of GO and TiO₂ sol was treated in a hydrothermal autoclave, GO was reduced to graphene. As shown in Fig. 2b, the peak of GO at 12.6° disappears, and all the main peaks can be assigned to anatase TiO₂. However, the XRD pattern of TiO₂/G nanocomposite should have a diffraction peak near to 26.5°, as graphene is multi-layered based on the TEM observation. Although the peak is absent in the XRD pattern of single-layer graphene, the absence of such peak for TiO₂/G nanocomposite should be the result of the overlap with the strong peak at 25.3° of anatase TiO₂. Such result suggests that GO was reduced to graphene and TiO₂/G nanocomposite was simultaneously formed under our hydrothermal conditions.

The XRD pattern of Ag/TiO₂/G nanocomposite is shown in Fig. 2c, which exhibits four additional peaks at 38.1°, 44.3°, 64.4°, and 77.4° compared with that of TiO₂/G nanocomposite. These peaks can be indexed to the cubic structure of Ag (JCPDS No. 65-2871), corresponding to (111), (200), (220), and (311) reflections, respectively. This result indicates that the metallic Ag nanoparticles were successfully anchored to TiO₂/G nanocomposite by reducing Ag⁺ ions with NaBH₄, forming an Ag/TiO₂/G nanocomposite. The average crystallite size of TiO₂ nanoparticles kept unaltered after the loading of Ag nanoparticles, based on the calculations by applying the Scherrer equation to the characteristic diffraction peaks.

Raman spectroscopic measurement was further to elucidate the structure of Ag/TiO₂/G nanocomposite. In general, the graphene sheet exhibits three most intense Raman bands at ~1350 cm⁻¹ (D band), ~1580 cm⁻¹ (G band), and ~2700 cm⁻¹ (2D band).²⁴ The D band is due to the breathing modes of sp² atoms in rings and is related to the occurrence of defects and structural disorder in graphene sheets. This band is absent in a defect-free graphene. The G band is derived from the stretching of the sp²-hybridized carbon-carbon bonds and is highly sensitive to strain effects in sp² system within graphene sheets. The 2D

band is the overtone of the D band and is sensitive to the number of graphene layers. The 2D band in multilayer graphene is much less intense and broader compared with the one in monolayer graphene.²⁵ These three characteristic bands were observed in all the samples, as indicated in Fig. 3. As evidenced in Fig. 3a, the as-prepared graphene is multi-layered since a strong D band and a weak 2D band were observed, which is consistent with the results of TEM and XRD analyses. A D/G intensity ratio near to 1.0 implies small average size of the sp^2 domains. An increment in D/G intensity ratio was observed in the Raman spectrum of TiO_2 /G nanocomposite, suggesting that an increase in the number of defects was brought by the introduction of TiO_2 nanoparticles on the graphene sheets,²⁶ possibly because that the formation of TiO_2 nanoparticles on graphene stressed its surface and induced more defects.

After the formation of TiO_2 /G nanocomposite, more additional Raman peaks around 143, 383, 501, and 626 cm^{-1} were found, which are ascribed to anatase TiO_2 . The result demonstrates that anatase TiO_2 was successfully attached to the graphene sheets. After the loading of Ag nanoparticles, there is no distinct change in the number of Raman peak as compared with that of TiO_2 /G nanocomposite. However, the intensity of Raman peaks of anatase TiO_2 increases intensively compared with that of graphene, which is associated with the surface enhancement effect on TiO_2 induced by the SPR effect of Ag nanoparticles. This fact further proves the existence of Ag nanoparticles in the Ag/TiO_2 /G nanocomposite. Because the Ag nanoparticles are deposited on the surface of TiO_2 nanoparticles, the Raman scattering of TiO_2 , not graphene, was notably enhanced by the SPR effect of Ag nanoparticles. However, the possibility of Ag nanoparticles deposited on the surface of graphene sheets cannot be completely excluded, as Ag^+ ions may react with the residual oxygen-containing functional groups because of the incomplete reduction of GO.

The C1s XPS spectra of GO and Ag/TiO_2 /G nanocomposite are shown in Fig. 4. In the deconvoluted C1s spectra of GO, the peak centered at 284.6 eV was attributed to the sp^2 or sp^3 carbon species, while the peaks at higher binding energies (286–290 eV) are

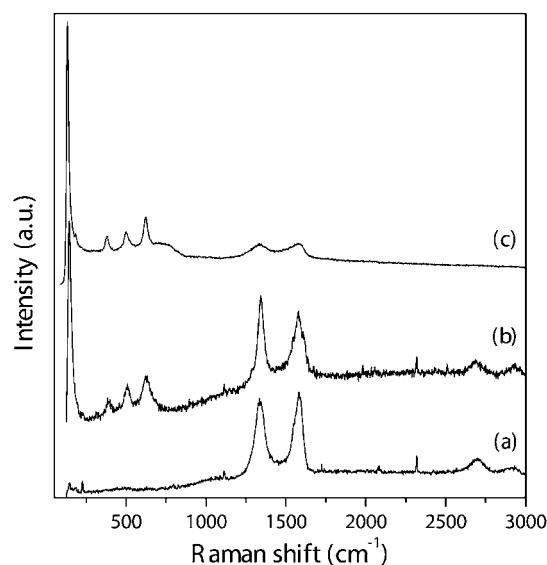


Fig. 3 Raman spectra of (a) graphene, (b) TiO_2 /G, and (c) Ag/TiO_2 /G.

assigned to oxygenated carbon species such as hydroxyl, epoxy, and carboxyl species on the GO surface.²⁷ After the formation of Ag/TiO_2 /G nanocomposite, the peak intensities of oxygenated carbon species decreased significantly, which suggests that GO was reduced to graphene. However, the residue of C=O species implies that a small part of carboxyl groups were kept under the hydrothermal conditions. These residual carboxyl groups could serve as a bridge between graphene and TiO_2 . Two peaks centered at 464.2 and 458.4 eV were observed in the Ti 2p XPS spectra of Ag/TiO_2 /G nanocomposite (figure not shown). They are ascribed to the Ti 2p_{1/2} and Ti 2p_{3/2} spin-orbit splitting states respectively, which are typical for TiO_2 .²⁸ The peak corresponding to Ti-C bonds at around 281 eV (C1s) was not observed, suggesting that there is no carbon doping in the lattice of TiO_2 or the formation of Ti-C bond between carbon of graphene sheets and TiO_2 .²⁹

The IR spectra of TiO_2 /G and Ag/TiO_2 /G nanocomposites are given in Fig. 5. As shown in Fig. 5a, two separate O-H stretching vibrational modes can be identified with principal absorption centered around 3418 and 3165 cm^{-1} in the IR spectrum of TiO_2 /G nanocomposite. The former band is the superposition of the O-H stretching vibrational modes of hydroxyl groups attached to graphene and anatase surfaces respectively. The latter one is attributed to the intercalated water within graphene sheets. The multiple bands appearing around 1635 cm^{-1} are assigned to the C-C vibrations of graphene sheets. The fundamental vibrations of anatase TiO_2 appear as very intensive broad bands over the range of 400–800 cm^{-1} , which are related to bending and stretching vibrational modes of Ti-O-Ti bonds (~ 670 and 571 cm^{-1}).³⁰ The vibrational bands of C-H and C-O bonds were identified in this spectrum, suggesting that GO was not completely reduced under the hydrothermal conditions. The peak at ~ 1000 cm^{-1} is assigned to the C-O stretching mode similar to the case of metal alkoxides. However, XRD measurements clearly indicated that TiO_2 is highly crystallized. Thus, one possibility is the formation of C-O-Ti bonds in the nanocomposite. The spectroscopic feature of Ag/TiO_2 /G nanocomposite is similar to that of TiO_2 /G, as indicated in Fig. 5, suggesting that the loading of Ag nanoparticles does not change the structure of TiO_2 /G nanocomposite.

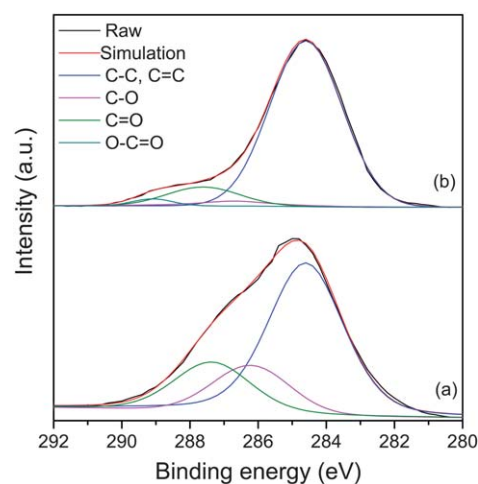


Fig. 4 C1s XPS spectra of (a) GO and (b) Ag/TiO_2 /G.

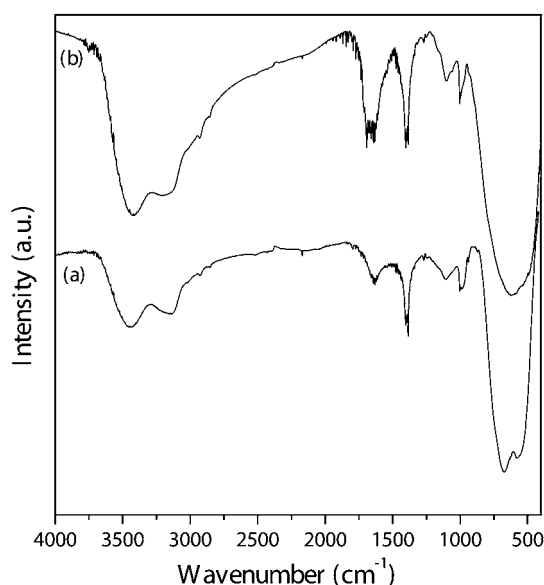


Fig. 5 IR spectra of (a) TiO_2/G and (b) $\text{Ag}/\text{TiO}_2/\text{G}$.

UV-vis spectroscopic measurement was carried out to examine the optical response of $\text{Ag}/\text{TiO}_2/\text{G}$ nanocomposite. As shown in Fig. 6, the absorption edge near 400 nm in all three samples is ascribed to the band-to-band transition of anatase TiO_2 . It is clearly seen that the absorption between 600 and 800 nm was enhanced when anatase TiO_2 and graphene formed a nanocomposite, as indicated by the dash line in Fig. 6. This absorption is due to the interaction between anatase TiO_2 nanoparticles and graphene sheets. Moreover, when Ag nanoparticles were introduced to form $\text{Ag}/\text{TiO}_2/\text{G}$ nanocomposite, a broad absorption band from 400 to 700 nm appeared. Such band is attributed to the SPR absorption of Ag nanoparticles, which further proves the successful introduction of Ag nanoparticles as result of the NaBH_4 reduction of Ag^+ ions. The broad

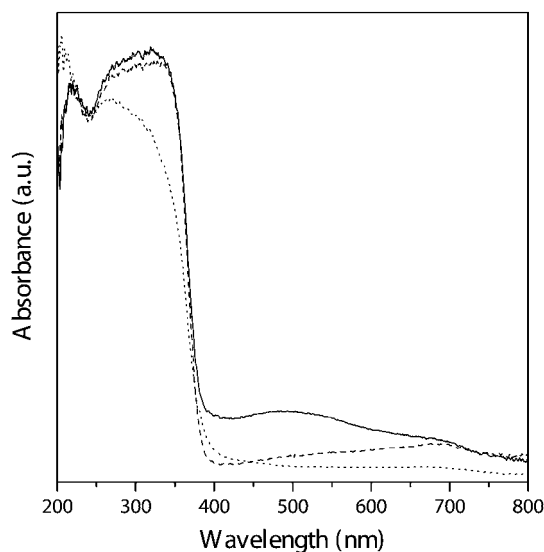


Fig. 6 UV-vis spectra of TiO_2 (dot line), TiO_2/G (dash line), and $\text{Ag}/\text{TiO}_2/\text{G}$ (solid line).

absorption of $\text{Ag}/\text{TiO}_2/\text{G}$ nanocomposite extending into the visible light region is expected to improve its photocatalytic activity under visible light irradiation.

3.2 Photocatalytic property of $\text{Ag}/\text{TiO}_2/\text{G}$ nanocomposite under visible light irradiation

The photocatalytic decolorization of methylene blue (MB) dye molecules was used to evaluate the photocatalytic performance of $\text{Ag}/\text{TiO}_2/\text{G}$ nanocomposite under visible light irradiation. Degussa P25 TiO_2 and TiO_2/G nanocomposite were chosen as the reference photocatalysts for comparison. The photocatalytic results are shown in Fig. 7. The MB molecules were strongly adsorbed by graphene, $\text{Ag}/\text{TiO}_2/\text{G}$, and TiO_2/G nanocomposites in the dark; however, there was no significant adsorption occurred on Degussa P25. It is clear to see that the strong adsorption of the MB molecules on two kinds of nanocomposites is due to the contribution of graphene, which has a large specific surface area and a strong affinity to the aromatic dye molecules via π - π interactions. The formation of nanocomposite will further increase the adsorption ability of graphene sheets because TiO_2 nanoparticles will separate the graphene sheets against the formation of aggregates due to the strong π - π interactions between themselves. The introduction of Ag nanoparticles has not side effect on the adsorption ability.

Under visible light irradiation, the MB molecules were slightly decolorized in the presence of graphene and Degussa P25. The reason for the former is the adsorption effect, and for the latter is the photosensitization effect. As the MB molecules can absorb visible light, electron transfer takes place from the photoexcited dye molecules to the TiO_2 conduction band under visible light irradiation. The dye molecules that have lost electrons will decompose if no sacrificial electron donor is available. However, the dye solution became nearly colorless in the presence of either

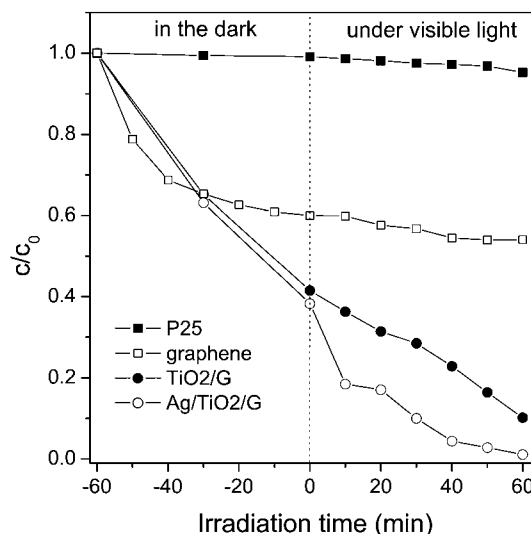


Fig. 7 Photocatalytic decolorization of methylene blue under visible light irradiation in the presence of P25 (■), graphene (□), TiO_2/G (●), and $\text{Ag}/\text{TiO}_2/\text{G}$ (○). c_0 is the initial concentration of the dye, and c is the concentration of the dye at time t . Reaction conditions: 0.1g of photocatalyst (0.01g for graphene), 100 ml of 10 mg mL^{-1} MB aqueous solution.

Ag/TiO₂/G or TiO₂/G nanocomposite after 60 min of visible light illumination. The complete decolorization can be mainly attributed to the photocatalytic reaction, rather than the adsorption or photosensitization effect, because both the effects have a very limited contribution as revealed in Fig. 7. As expected, Ag/TiO₂/G nanocomposite showed better photocatalytic activity than TiO₂/G nanocomposite, as presented in Fig. 7.

Several efforts have been made to prepare TiO₂/graphene nanocomposites and explore their photocatalytic properties.^{11–15} Their highly photocatalytic activities under visible light irradiation have been explained due to the unique electric property of graphene and the interaction between TiO₂ and graphene.^{13,14} However, the underlying mechanism is not well understood currently. Some researchers suggested that graphene should act as a sensitizer for light absorption to produce the photogenerated electrons, which are subsequently injected into the TiO₂ conduction band, similar to the case in TiO₂/carbon nanotube nanocomposites.³¹ Pristine graphene is a zero band gap semiconductor and has a work function of 4.42–4.66 eV.^{32,33} Graphene obtained from the reduction of GO should have a higher work function than the pristine one due to the possible incomplete reduction.³⁴ Since the electron affinity of anatase TiO₂ (~4.2 eV) is lower than the work function of graphene, electron transfer from the TiO₂ conduction band to graphene is energetically favorable.³⁵ The successful photocatalytic reduction of GO to graphene under UV light irradiation also proven that the photoexcited electrons were transferred from the TiO₂ conduction band to GO.^{8,36} Thus, the explanation of graphene as a role of a sensitizer is not reasonable. Others argued that the formation of C–Ti–O bonds extends the light absorption to longer wavelengths, similar to the case of carbon-doped TiO₂.^{13,37,38} Most recently, the *ab initio* calculations confirmed that several energy states exist in the middle of band gap of TiO₂ due to the hybridization of C_{2p} with O_{2p} or Ti_{3d} orbitals.³⁹ The transition from these surface states close to the valence band maximum to the states near to the conduction band minimum or the conduction band itself should be responsible for the visible light response of TiO₂/G nanocomposite. Since the surface states in the band gap are limited by the amount of C–Ti–O bonds, the absorbance in the visible light region is expected to be restricted. This assumption is consistent with the results of UV–vis spectroscopic measurements, as shown in Fig. 6. The anodic shift of flat-band potential of TiO₂/graphite-like carbon compared with P25 based on Mott-Schottky measurements also supported this hypothesis.⁴⁰ Thus, this explanation is more sensible to explain the origin of visible light absorption for TiO₂/G nanocomposite, but the true mechanism may be more complicated.

In the case of Ag/TiO₂/G nanocomposite, a Schottky junction is formed between Ag and TiO₂ once they come into contact because Fermi level of TiO₂ is higher than that of Ag.⁴¹ The formation of a Schottky barrier will hinder electrons across the boundary transferring from Ag to TiO₂. However, the electron injection from Ag to TiO₂ on SPR excitation has been proven truly happened in Au/TiO₂ and Ag/TiO₂ systems,^{6,42–44} although the detailed mechanism on such transferal is still unclear at present. One possible explanation suggested that electrons oscillating collectively on the SPR excitation might lead to interband excitation, giving enough energy to electrons moving to the interface to overcome the Schottky barrier on Ag/TiO₂,

which is only 0.4 eV above the Fermi level.^{43,44} Once the SPR excited electrons are transferred to the TiO₂ conduction band, they are subsequently trapped by the adsorbed molecular oxygen on the TiO₂ surface producing superoxide anion radicals ($\cdot\text{O}_2^-$). Furthermore, these electrons can transfer from the TiO₂ conduction band to the graphene sheets as mentioned above. The two-dimensional planar conjugation structure in graphene facilitates interfacial charge transfer along the graphene sheets to any electron acceptors like oxygen molecules, and subsequently an effective charge separation is achieved. If graphene was not perfectly restored from GO during the reduction process, any defects on graphene sheets would depress the charge separation efficiency, thus diminish the photocatalytic activity of the nanocomposite. At the same time, the oxidized Ag species accept electrons from H₂O or hydroxide ions adsorbed on the TiO₂ surface or from the dye molecules present in the solution and are regenerated. The reaction with H₂O or hydroxide ions produces hydroxyl radicals ($\cdot\text{OH}$). These radicals ($\cdot\text{O}_2^-$ and $\cdot\text{OH}$) are very powerful oxidizing agents for the degradation of MB molecules. As a result, the separated holes and electrons can be fully involved in the photocatalytic reactions, and a highly efficient photocatalytic activity is expected. The proposed mechanism for the photocatalytic degradation of organic dyes under visible light irradiation is illustrated in Fig. 8.

In order to meet the requirements for practical applications, a good photocatalyst should have high photocatalytic activity and good stability. In order to test the photocatalytic stability of Ag/TiO₂/G nanocomposite, the photocatalyst was recycled up to five times. As shown in Fig. 9, its photocatalytic activity was slightly deteriorated after five consecutive photocatalytic experiments, accompanied with the decreased adsorption capacity. As TiO₂ and Ag nanoparticles are not uniformly distributed on the surface of the graphene sheets, the dye molecules adsorbed on the sites where no TiO₂ nanoparticle is deposited will be not degraded. They are also not easily washed away when the photocatalyst is regenerated for the next run because of the interactions between the graphene sheets and the dye molecules. As a result, the existence of these dye molecules on the graphene sheets will reduce the adsorption capacity towards the fresh dye solution, and subsequently decrease the photocatalytic efficiency during the same reaction period. This result indicated that Ag/TiO₂/G nanocomposite almost retained its photocatalytic activity in the repeated photocatalytic runs.

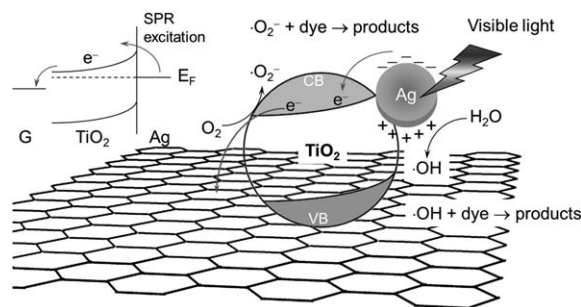


Fig. 8 Proposed mechanism for the photocatalytic degradation of organic dyes over Ag/TiO₂/G nanocomposite under visible light irradiation.

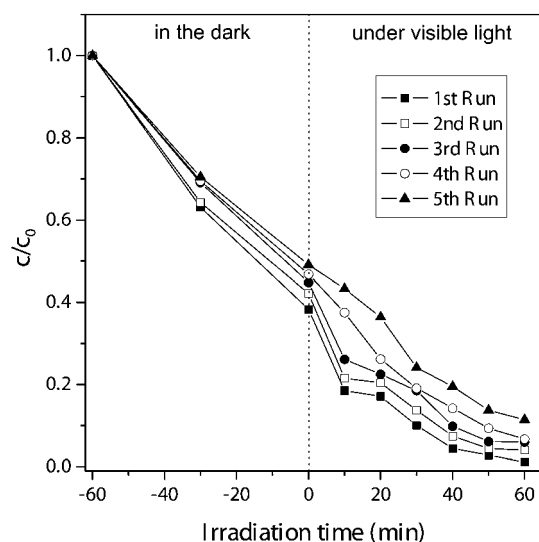


Fig. 9 Photocatalytic decolorization of MB under visible light irradiation over Ag/TiO₂/G nanocomposite recycled five times. Reaction conditions: 0.1 g of photocatalyst, 100 ml of 10 mg mL⁻¹ MB aqueous solution.

4. Conclusion

In this work, we have demonstrated a new strategy by utilizing the excellent electrical properties of graphene and the SPR effect of noble metallic nanoparticles to increase the photocatalytic efficiency of TiO₂. A photocatalyst of Ag/anatase TiO₂/graphene nanocomposite was prepared following such idea, which exhibited enhanced photocatalytic activity in the degradation of methylene blue molecules under visible light irradiation. The enhanced photocatalytic activity is associated with wide visible light response and high electron-hole separation efficiency due to the synergetic interactions between TiO₂, graphene and Ag. The coupling of graphene to improve the photocatalytic activity of TiO₂ could be applied to other wide band gap semiconductor materials, while the introduction of noble metallic nanoparticles can further boost the photocatalytic efficiency. Since the SPR effect of noble metallic nanoparticles strongly depends on their species, size and shape, the optical response of nanocomposites of graphene and wide band gap semiconductors can be flexibly tuned, thereby further extending their absorption of sunlight and enhancing their photocatalytic activity.

Acknowledgements

This work was supported by the National Natural Science Foundation of China (Grant No. 20971044).

References

- X. Chen and S. S. Mao, *Chem. Rev.*, 2007, **107**, 2891–2959.
- H. M. Sung-Suh, J. R. Choi, H. J. Hah, S. M. Koo and Y. C. Bae, *J. Photochem. Photobiol., A*, 2004, **163**, 37–44.
- M. Andersson, H. Birkedal, N. R. Franklin, T. Ostomel, S. Boettcher, A. E. C. Palmqvist and G. D. Stucky, *Chem. Mater.*, 2005, **17**, 1409–1415.
- M. R. Elahifard, S. Rahimnejad, S. Haghighi and M. R. Gholami, *J. Am. Chem. Soc.*, 2007, **129**, 9552–9553.
- Y. Li, H. Zhang, Z. Guo, J. Han, X. Zhao, Q. Zhao and S.-J. Kim, *Langmuir*, 2008, **24**, 8351–8357.

- K. Awazu, M. Fujimaki, C. Rockstuhl, J. Tominaga, H. Murakami, Y. Ohki, N. Yoshida and T. Watanabe, *J. Am. Chem. Soc.*, 2008, **130**, 1676–1680.
- K. Woan, G. Pyrgiotakis and W. Sigmund, *Adv. Mater.*, 2009, **21**, 2233–2239.
- G. Williams, B. Seger and P. V. Kamat, *ACS Nano*, 2008, **2**, 1487–1491.
- C. Nethravathi and M. Rajamathi, *Carbon*, 2008, **46**, 1994–1998.
- T. N. Lambert, C. A. Chavez, B. Hernandez-Sanchez, P. Lu, N. S. Bell, A. Ambrosini, T. Friedman, T. J. Boyle, D. R. Wheeler and D. L. Huber, *J. Phys. Chem. C*, 2009, **113**, 19812–19823.
- O. Akhavan and E. Ghaderi, *J. Phys. Chem. C*, 2009, **113**, 20214–20220.
- X.-Y. Zhang, H.-P. Li, X.-L. Cui and Y. Lin, *J. Mater. Chem.*, 2010, **20**, 2801–2801.
- H. Zhang, X. Lv, Y. Li, Y. Wang and J. Li, *ACS Nano*, 2010, **4**, 380–386.
- Y. Zhang, Z.-R. Tang, X. Fu and Y.-J. Xu, *ACS Nano*, 2010, **4**, 7303–7314.
- Y. H. Ng, I. V. Lightcap, K. Goodwin, M. Matsumura and P. V. Kamat, *J. Phys. Chem. Lett.*, 2010, **1**, 2222–2227.
- R. Pasricha, S. Gupta and A. K. Srivastava, *Small*, 2009, **5**, 2253–2259.
- X. Zhou, X. Huang, X. Qi, S. Wu, C. Xue, F. Y. C. Boey, Q. Yan, P. Chen and H. Zhang, *J. Phys. Chem. C*, 2009, **113**, 10842–10846.
- J. Li and C.-y. Liu, *Eur. J. Inorg. Chem.*, 2010, 1244–1248.
- X.-Z. Tang, Z. Cao, H.-B. Zhang, J. Liu and Z.-Z. Yu, *Chem. Commun.*, 2011, **47**, 3084–3086.
- T. Wu, S. Liu, Y. Luo, W. Lu, L. Wang and X. Sun, *Nanoscale*, 2011, **3**, 2142–2144.
- W. S. Hummers and R. E. Offeman, *J. Am. Chem. Soc.*, 1958, **80**, 1339–1339.
- N. I. Kovtyukhova, P. J. Ollivier, B. R. Martin, T. E. Mallouk, S. A. Chizhik, E. V. Buzaneva and A. D. Gorchinskiy, *Chem. Mater.*, 1999, **11**, 771–778.
- Y. Zhou, Q. Bao, L. A. L. Tang, Y. Zhong and K. P. Loh, *Chem. Mater.*, 2009, **21**, 2950–2956.
- A. C. Ferrari, *Solid State Commun.*, 2007, **143**, 47–57.
- Y. y. Wang, Z. h. Ni, T. Yu, Z. X. Shen, H. m. Wang, Y. h. Wu, W. Chen and A. T. Shen Wee, *J. Phys. Chem. C*, 2008, **112**, 10637–10640.
- B. Krauss, T. Lohmann, D. H. Chae, M. Haluska, K. von Klitzing and J. H. Smet, *Phys. Rev. B: Condens. Matter Mater. Phys.*, 2009, **79**, 165428.
- S. Yumitori, *J. Mater. Sci.*, 2000, **35**, 139–146.
- E. McCafferty and J. P. Wightman, *Surf. Interface Anal.*, 1998, **26**, 549–564.
- H. Irie, Y. Watanabe and K. Hashimoto, *Chem. Lett.*, 2003, **32**, 772–773.
- N. T. McDevitt and W. L. Baun, *Spectrochim. Acta*, 1964, **20**, 799–808.
- W. Wang, P. Serp, P. Kalck and J. L. Faria, *J. Mol. Catal. A: Chem.*, 2005, **235**, 194–199.
- R. Czerw, B. Foley, D. Tekleab, A. Rubio, P. Ajayan and D. Carroll, *Phys. Rev. B: Condens. Matter*, 2002, **66**, 033408.
- Y. Shi, K. K. Kim, A. Reina, M. Hofmann, L.-J. Li and J. Kong, *ACS Nano*, 2010, **4**, 2689–2694.
- C. Chen, W. Cai, M. Long, B. Zhou, Y. Wu, D. Wu and Y. Feng, *ACS Nano*, 2010, **4**, 6425–6432.
- Y.-B. Tang, C.-S. Lee, J. Xu, Z.-T. Liu, Z.-H. Chen, Z. He, Y.-L. Cao, G. Yuan, H. Song, L. Chen, L. Luo, H.-M. Cheng, W.-J. Zhang, I. Bello and S.-T. Lee, *ACS Nano*, 2010, **4**, 3482–3488.
- Y. H. Ng, A. Iwase, N. J. Bell, A. Kudo and R. Amal, *Catal. Today*, 2011, **164**, 353–357.
- G. Pyrgiotakis, S.-H. Lee and W. Sigmund, presented in part at the MRS Spring Meeting, San Francisco, CA, 2005.
- Y. Zhang and C. Pan, *J. Mater. Sci.*, 2010, **46**, 2622–2626.
- A. Du, Y. H. Ng, N. J. Bell, Z. Zhu, R. Amal and S. C. Smith, *J. Phys. Chem. Lett.*, 2011, **2**, 894–899.
- L.-W. Zhang, H.-B. Fu and Y.-F. Zhu, *Adv. Funct. Mater.*, 2008, **18**, 2180–2189.
- A. Sclafani and J.-M. Herrmann, *J. Photochem. Photobiol., A*, 1998, **113**, 181–188.
- Y. Tian and T. Tatsuma, *J. Am. Chem. Soc.*, 2005, **127**, 7632–7637.
- J. Okumu, C. Dahmen, A. N. Sprafke, M. Luysberg, G. von Plessen and M. Wuttig, *J. Appl. Phys.*, 2005, **97**, 094305.
- A. Furube, L. Du, K. Hara, R. Katoh and M. Tachiya, *J. Am. Chem. Soc.*, 2007, **129**, 14852–14853.